

## Electronic Supplementary Information

### **K<sub>2</sub>V<sub>6</sub>O<sub>16</sub>•2.7H<sub>2</sub>O nanorod cathode: an advanced intercalation system for high energy aqueous rechargeable Zn-ion batteries†**

Balaji Sambandam<sup>a‡</sup>, Vaiyapuri Soundharrajan<sup>a‡</sup>, Sungjin Kim<sup>a</sup>, Muhammad H. Alfaruqi<sup>ab</sup>, Jeonggeun Jo<sup>a</sup>, Seokhun Kim<sup>a</sup>, Vinod Mathew<sup>a</sup>, Yang-kook Sun<sup>c</sup> and Jaekook Kim<sup>a\*</sup>

<sup>a</sup>Department of Materials Science and Engineering, Chonnam National University, 300Yongbong-dong, Bukgu, Gwangju 500-757, South Korea.

<sup>b</sup>Metallurgy Department, Sumbawa University of Technology, Jl. Raya Olat Maras, Sumbawa, West Nusa Tenggara 84371, Indonesia

<sup>c</sup>Department of Energy Engineering, Hanyang University, Seoul 133-791, South Korea.

E-mail: jaekook@chonnam.ac.kr; Fax: +82-62-530-1699; Tel: +82-62-530-1703.

‡ These authors contributed equally

## Experimental section

### Material Preparation

KOH (1 mmol) and  $V_2O_5$  (1 mmol) were dissolved in deionized (DI) water. After stirring for a few minutes, the mixture was transferred to a 50-mL Teflon-lined autoclave, filled to 70% capacity. The autoclave was sealed, placed in an oven, heated at 200 °C for 24 h, and allowed to cool naturally. The final products were washed several times with distilled water and ethanol and dried in an oven at 70 °C for 8 h to obtain phase-pure KVO. The as-synthesized powder was sampled directly for further characterizations.

### Material characterization

Powder X-ray powder diffraction measurements (PXRD, Cu  $K\alpha$  radiation, with  $\lambda = 1.5406$  Å) were carried out using a Shimadzu X-ray diffractometer. The surface morphology was analyzed by field-emission scanning electron microscopy (FE-SEM) using S-4700 Hitachi with an energy-dispersive X-ray spectroscopy (EDS) detector. The lattice fringes were analyzed using a field-emission transmission electron microscope (FE-TEM, Philips Tecnai F20 at 200 kV). The elemental oxidation states were examined by X-ray photoelectron spectroscopy (XPS, Thermo VG Scientific Instruments, Multilab 2000) using Al  $K\alpha$  as the X-ray source. The spectrometer was calibrated relative to the C 1s peak binding energy of 284.6 eV. The elemental compositions of the sample were determined via ICP-OES (inductively coupled plasma-optical emission spectroscopy) analysis using a Perkin Elmer 4300 DV analyzer. Thermogravimetric analysis (TGA) using an SDT Q600 thermobalance in nitrogen atmosphere with a temperature change of 5 °C  $\text{min}^{-1}$  was performed to understand the stability of the material.

### Electrochemical characterization

A paste of 70, 20, and 10 wt% of the active material, Ketjen black, and Teflonated acetylene black (TAB), respectively, were pressed onto a stainless-steel mesh before vacuum drying at 120 °C for 12 h. The mass load of the active material is 3 mg. Zn metal foil and a 1M  $ZnSO_4$  solution were used as the anode and electrolyte, respectively. While preparing 2032-type coin cells, a glass-fiber separator soaked with the electrolyte was pressed between the prepared cathode and the anode in open-air conditions and aged for 12 h before performing electrochemical discharge/charge measurements using a BTS 2004H model (NAGANO, Japan) battery tester at different current densities between 0.4 and 1.4 V vs.  $Zn^{2+}/Zn$ . For the cyclic voltammetry (CV) scans along with simultaneous measurements of electrochemical impedance spectroscopy (EIS), an AUTOLAB PGSTAT302N potentiostat model workstation was used.

The specific energy is calculated based on specific capacity and voltage (potential at which 50% of discharge capacity is reached).<sup>17</sup> More information can be found in supplementary data.

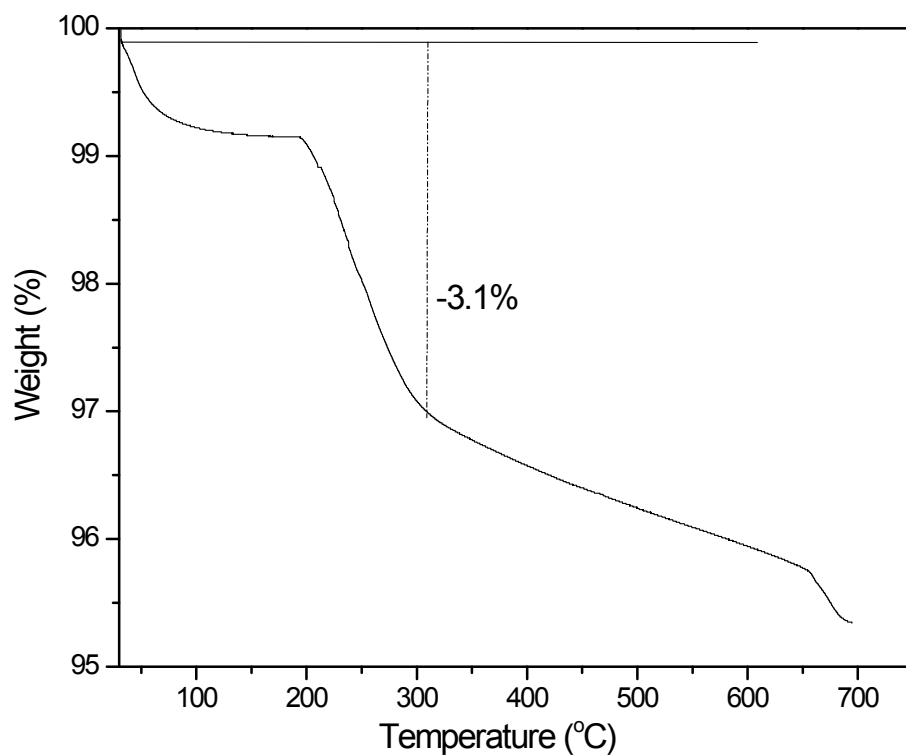


**Fig. S1.** TG analysis of KVO nanorods under nitrogen atmosphere with temperature ramp of 5 °C/min. Nanorods showing stepwise loss of water molecules with corresponding weight loss of 3.1%, equivalent to 2.46 molecule of water per unit formula.

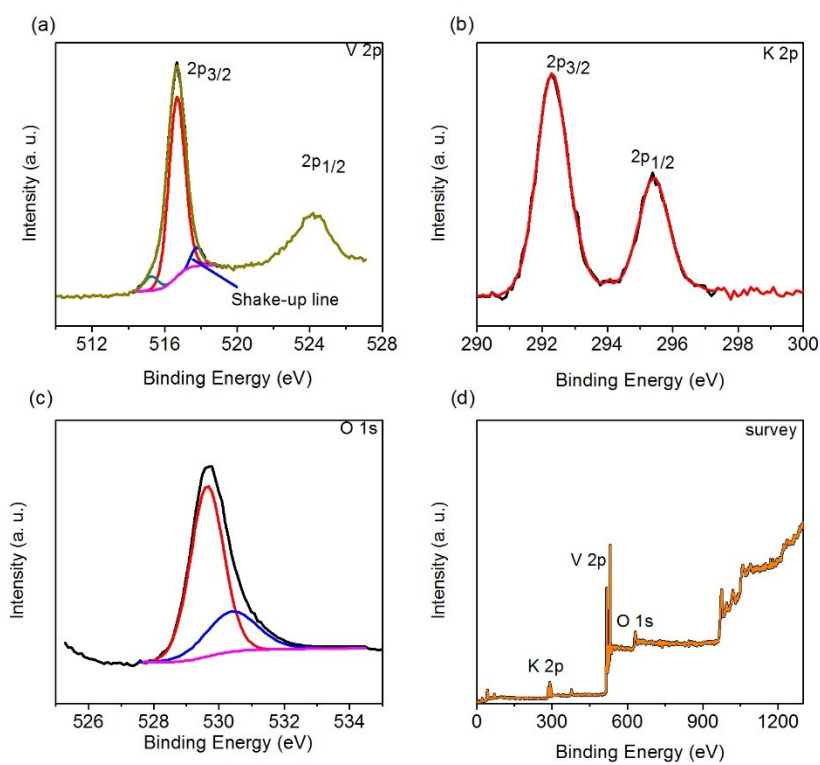


**Fig. S2.** XPS profiles for KVO as prepared sample (a) V 2p, (b) K 2p, (c) O 1s and (d) survey spectral line.

**Table S1.** ICP data for pristine sample

S. No	Elements	Concentration (wt%)
1	K	8.75
2	V	33.9

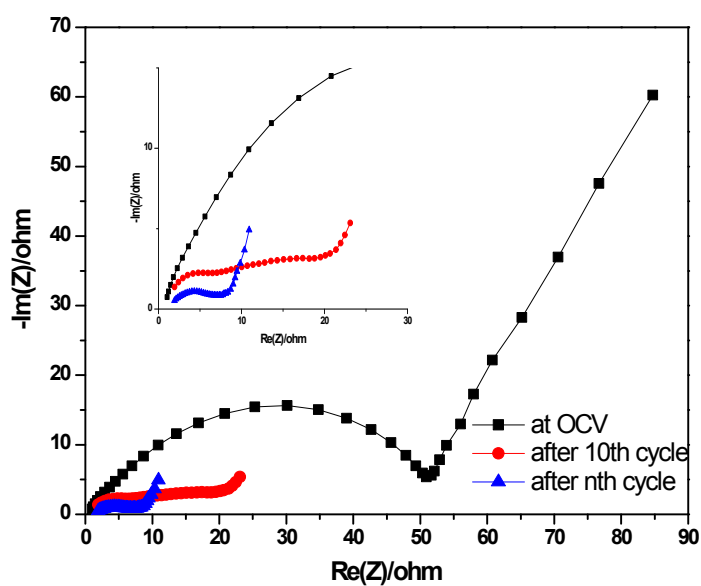


**Fig. S3.** In situ EIS measurements (Nyquist plots) for before and after cycling of KVO cathode for ARZIBs. Inset: magnified region.

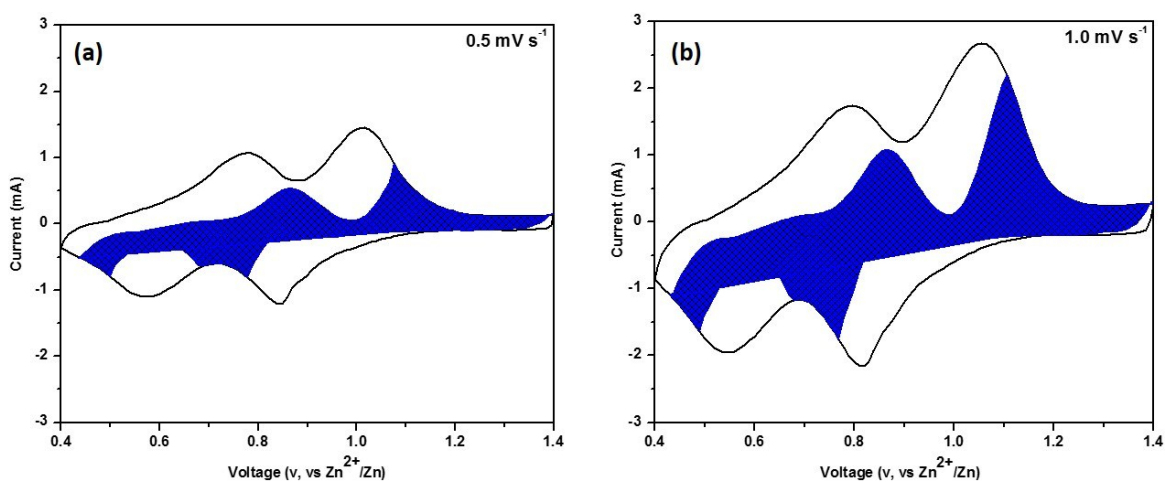


**Fig. S4.** The contribution ratio of the capacitive capacities and diffusion-limited capacities based on equation 2 at (a) 0.5 and (b) 1.0  $\text{mV s}^{-1}$ .

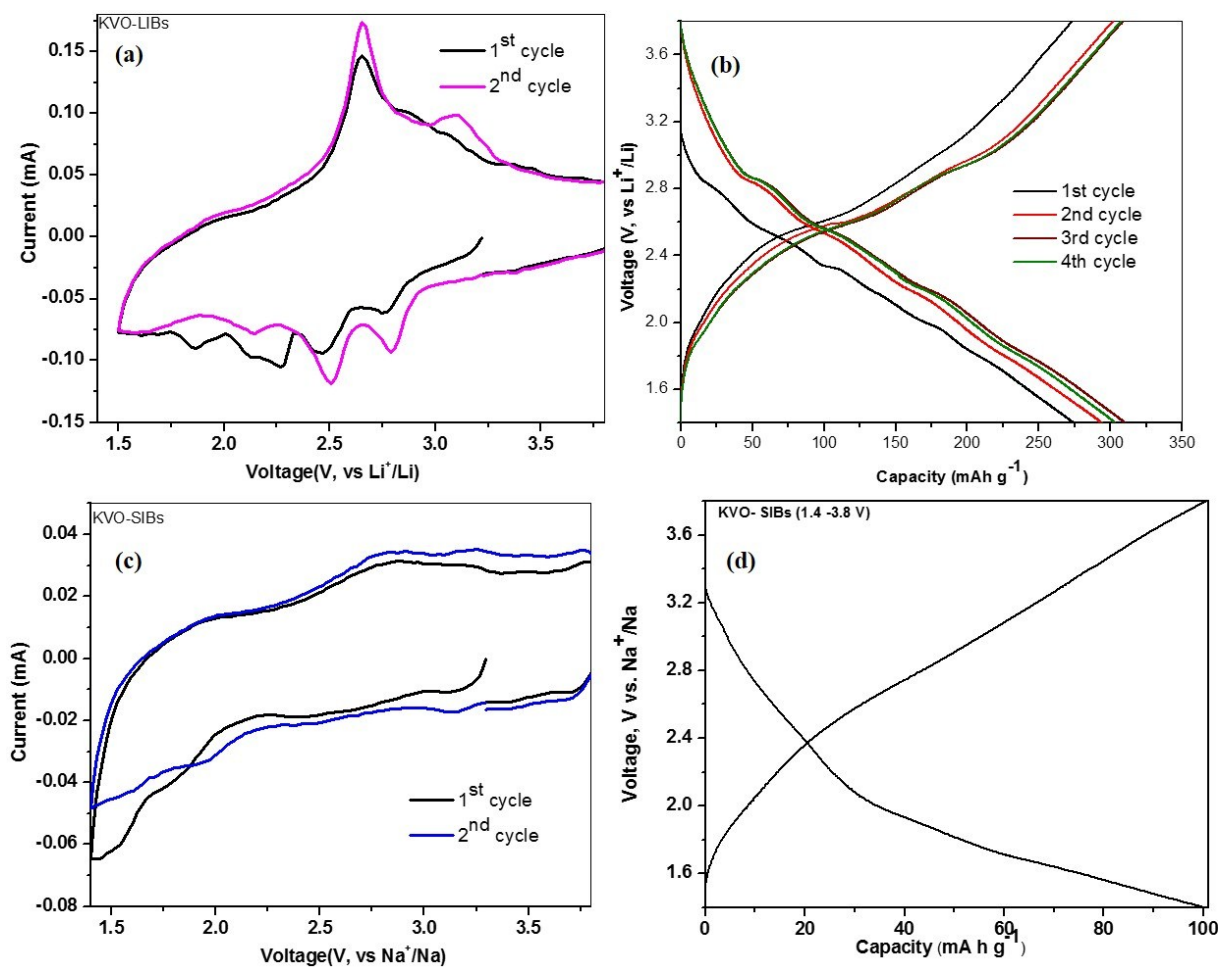


**Fig. S5.** KVO cathode (a) CV at 0.2 mV s<sup>-1</sup> and (b) ECD patterns at 50 mA g<sup>-1</sup> for LIBs, (c) CV at 0.2 mV s<sup>-1</sup> (d) ECD patterns at 50 mA g<sup>-1</sup> for SIBs.

### Electrochemical measurements

A mixture of active material, Super P as conducting carbon, and a polyacrylic acid binder in N-methyl-2-pyrrolidone (NMP) to form a slurry at a weight ratio of 70:20:10 which serve as a working electrode. The active material loading was found to be 1.2–1.4 mg. It was then uniformly coated on a pure Al foil, which acts as a current collector, and dried overnight under vacuum at 120 °C. The dried foil was pressed between stainless steel twin rollers and then punched into circular discs.

**For Li half-cell:** The cell assembled in glovebox with 2032 coin-type cells using Li foil as the counter electrode along with a membrane (Celgard 2400) as a separator. The electrolyte was 1 M LiPF<sub>6</sub> in ethylene carbonate:dichloromethane (1:1 by volume).

**For Na half-cell:** The cell assembled in glovebox with 2032 coin-type cells using Na foil as the counter electrode along with a glass filter separator. The electrolyte was 1 M NaPF<sub>6</sub> in 1:1 volume ratio of ethylene carbonate (EC) and propylene carbonate (PC), respectively, and 2% fluoroethylene carbonate.

Electrochemical studies were performed on a BTS-2004H (Nagano, Japan) battery test instrument at 1.4–3.8 V after aging them for 12 h. CV measurement were performed using a Bio Logic Science Instrument (VSP 1075) at 0.2 mV s<sup>-1</sup> scan rate.

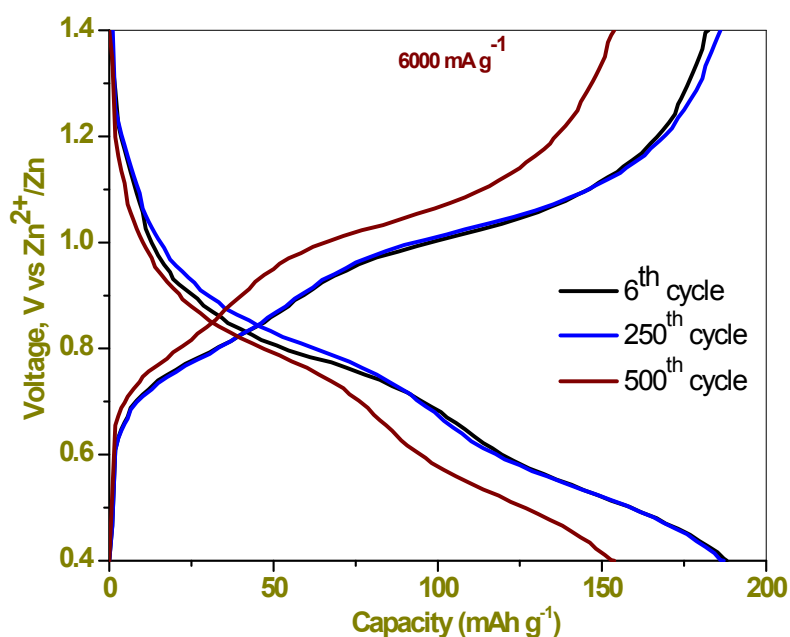


**Fig. S6.** Selected electrochemical discharge-charge depths at 6 A g<sup>-1</sup> current density over 1000 cycles for KVO nanorods.

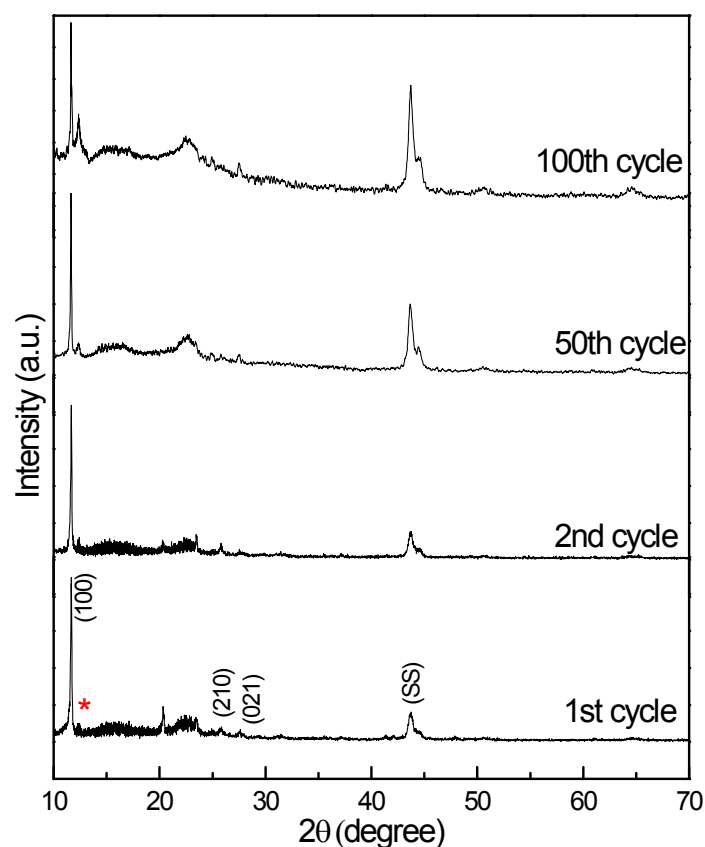


**Fig. S7.** Ex situ XRD patterns at different cycles end. The detailed preparation method of the slurry-based electrode and the electrochemical measurement conditions were given below.

**Electrochemical Measurements.** A CR 2032-type half-cell was assembled by using the KVO electrode with zinc metal as counter and reference electrode in an aqueous 1M ZnSO<sub>4</sub> electrolyte. Briefly, the working electrodes were prepared by mixing the active material (80%), Super P (10%), 5 wt % aqueous solution of sodium carboxymethyl cellulose (CMC, at 4%), and 50 wt% aqueous solution of styrene-butadiene rubber (SBR, at 6%). An optimized amount of distilled water was then added and mixed in a Spex ball mill for 10 min to obtain a homogeneous slurry, which was then uniformly coated onto a stainless steel foil current collector.

**Ex situ XRD analysis.** The ex situ XRD at different cycles end describes the phase stability of KVO electrode for ARZIBs. Few planes of KVO material are resolved, as represented in Fig. S7, and the  $2\theta$  region between 13-22° are well occupied by carbon sources. It is worth noting here that the cycled KVO electrode used for the XRD measurement was actually fabricated by



using the slurry method unlike the usual case of paste-type KVO electrode used for ex-situ XRD studies performed at different discharge/charge depths of the initial cycle and discussed in detail in the main text (Fig. 5b-c). Hence, the ex situ XRD patterns in Fig. S7 and Fig 5b reveal active material peaks that are in good agreement with each other whereas these patterns display differences in the carbon peak positions due to the fact that the carbon sources used for making the slurry (Super P and CMC-SBR) are different from those used for making the paste (Ketjen black and TAB). Nevertheless, the carbon and active material peak features in Fig. S7 are well resolved for the cathode patterns obtained after the 50 and 100<sup>th</sup> cycle. Interestingly, a new plane at 12.3° in all cycles (represented by \*), corresponding to the formation/dissolution of  $Zn_4(OH)_6SO_4 \cdot 0.5H_2O$  during discharge/charge processes, is observed. This phase is not completely dissolved during postmortem analysis and its origin is from the  $Zn_4(OH)_6SO_4 \cdot 5H_2O$  compound which lost part of the lattice water molecules during the process of drying at 120 °C. The formation/dissolution of  $Zn_4(OH)_6SO_4 \cdot 5H_2O$  ( $Zn_4(OH)_6SO_4 \cdot 0.5H_2O$ ) is partially resolved in Fig. 5c (0.4 V at the end of discharge and 0.8 V at the beginning of charge) of the main text.

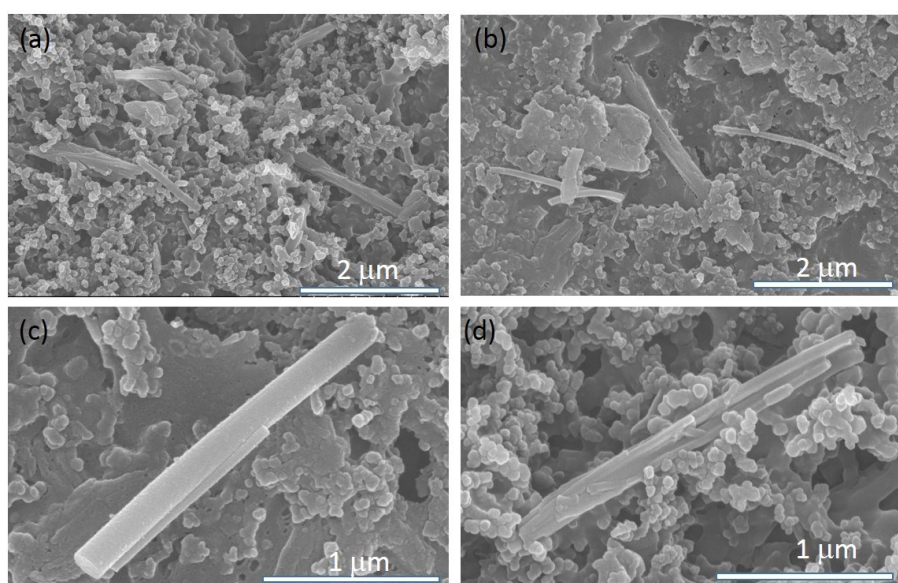


**Fig. S8.** Ex situ SEM images at different end cycles of (a) 1<sup>st</sup>, (b) 2<sup>nd</sup>, (c) 50<sup>th</sup> and (d) 100<sup>th</sup> for ARZIBs using KVO cathode.

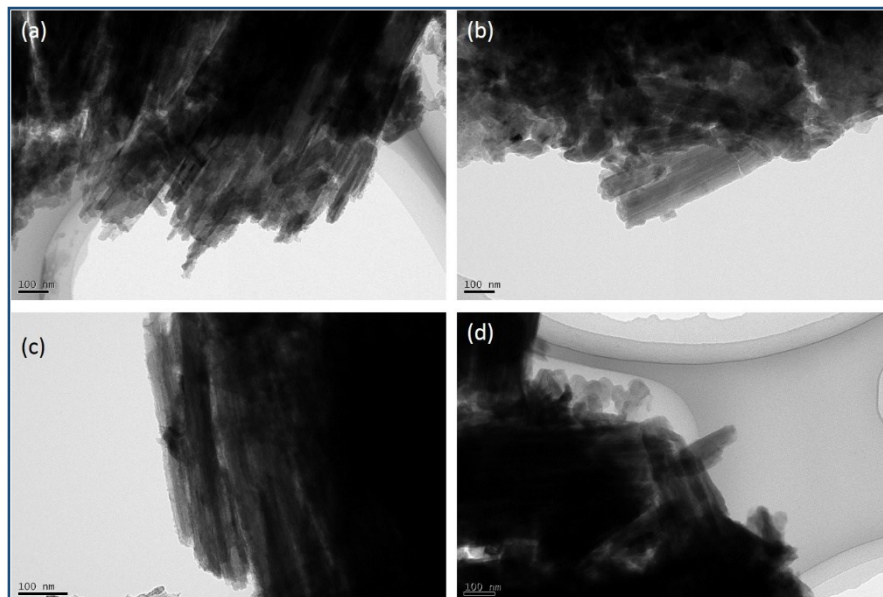


**Fig. S9.** Ex situ TEM images at different end cycles of (a) 1<sup>st</sup>, (b) 2<sup>nd</sup>, (c) 50<sup>th</sup> and (d) 100<sup>th</sup> for ARZIBs using KVO cathode.

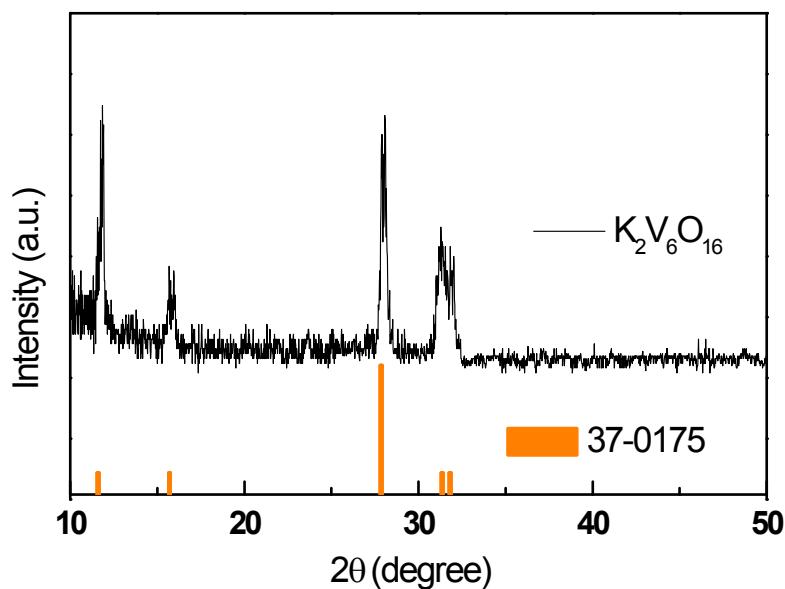


**Fig. S10.** XRD profile of anhydrous KVO obtained after annealing the K<sub>2</sub>V<sub>6</sub>O<sub>16</sub>·2.7H<sub>2</sub>O sample in air at 320 °C.

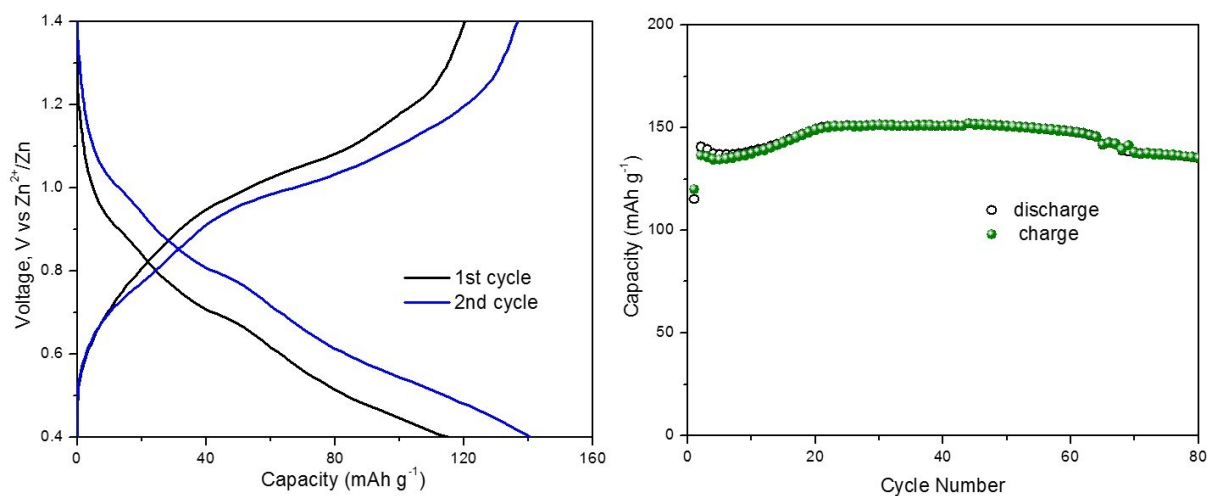


**Fig. S11.** (a) ECD profiles of anhydrous KVO for initial two cycles and (b) corresponding cyclability curve at a 200 mA g<sup>-1</sup> of applied current drain.

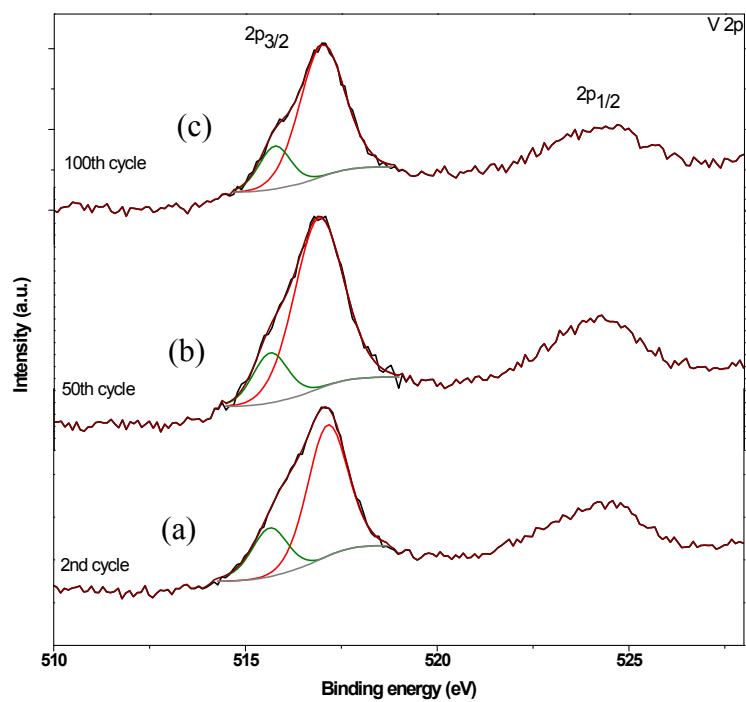


**Fig. S12.** Ex situ XPS V 2p line at different end cycles of (a) 2<sup>nd</sup>, (b) 50<sup>th</sup> and (c) 100<sup>th</sup> for ARZIBs using KVO cathode.

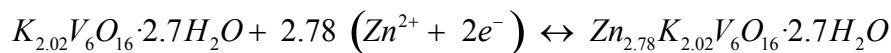
### Calculation of number of mole of Zn-insertion (n) in KVO

The number of electrons involved for zinc intercalation can thus be calculated based on two electron redox center of vanadium.<sup>1</sup> Thus the electrochemical reaction of  $K_2V_6O_{16} \cdot 2.7H_2O$  allows an intercalation of maximum 6 moles of  $Zn^{2+}$  ions per unit formula ( $Zn_6K_2V_6O_{16} \cdot 2.7H_2O$ ), the corresponding theoretical capacity being estimated to be 466.58 mAh  $g^{-1}$ .

This theoretical capacity calculation is estimated based on the Faraday equation given below

$$n = \frac{Q(\text{mAhg}^{-1}) \cdot MW(\text{gmol}^{-1})}{F(\text{mAhmol}^{-1})}$$

where n is number of electrons involved, Q is specific capacity, MW is molecular weight and F is Faraday constant. Thus, for the observed specific capacity of 329.6 (216.9) mAh  $g^{-1}$  at 53rd (1st) cycle end, it can be estimated from the above equation that nearly 8.48 (5.57) electrons are involved in the electrochemical reaction. This implies that 4.24 (2.78) mol of Zn-ions can be intercalated per KVO formula unit at 53rd (1st) cycle end. The overall reaction at first cycle can thus be written as below:



### Specific power and specific energy calculation:

Specific power (W  $Kg^{-1}$ ):  $I \cdot V / 2m$

Where I is the applied current (A), V is the cell voltage (V), m is the total active mass at cathode (g).<sup>2,3</sup>

Specific energy (Wh  $Kg^{-1}$ ): specific capacity \* voltage (potential at which 50% of discharge capacity is reached)

### References

1. N. Zhang, Y. Dong, M. Jia, X. Bian, Y. Wang, M. Qiu, J. Xu, Y. Liu, L. Jiao, F. Cheng, *ACS Energy Lett.*, 2018, **3**, 1366–1372.
- R. Thangavel, B. Moorthy, D.K. Kim, Y.S. Lee, *Adv. Energy Mater.*, 2017, **7**, 1602654.
2. M.D. Stoller, R.S. Ruoff, *Energy Environ. Sci.*, 2010, **3**, 1294-1301.

3. Y. Zhu, S. Murali, M.D. Stoller, K.J. Ganesh, W. Cai, P.J. Ferreira, A. Pirkle, R.M. Wallace, A. Cychoz, M. Thommes, D. Su, E.A. Stach, R.S. Ruoff, *Science*, 2011, **332**, 1537-1541.